Radiotherapy and Oncology 135 (2019) 78–85

Contents lists available at ScienceDirect

Radiotherapy and Oncology

journal homepage: www.thegreenjournal.com

Original Article

Ultrafast single breath-hold cone-beam CT lung cancer imaging with faster linac gantry rotation

Anna Arns [a,b,*], Hansjoerg Wertz [a], Judit Boda-Heggemann [a], Frank Schneider [a], Manuel Blessing [a], Yasser Abo-Madyan [a], Volker Steil [a], Frederik Wenz [a], Jens Fleckenstein [a]

[a] Department of Radiation Oncology, University Medical Center Mannheim, University of Heidelberg, Mannheim, Germany; [b] Department of Medical Physics and Bioengineering, Christchurch Hospital, Christchurch, New Zealand

ARTICLE INFO

Article history:
Received 15 September 2018
Received in revised form 1 February 2019
Accepted 3 February 2019
Available online 16 March 2019

Keywords:
IGRT
CBCT
Single breath-hold imaging
Ultrafast imaging
Lung DIBH

ABSTRACT

Purpose: Lung tumors treated with hypo-fractionated deep-inspiration breath-hold stereotactic body radiotherapy benefit from fast imaging and treatment. Single breath-hold cone-beam-CT (CBCT) could reduce motion artifacts and improve treatment precision. Thus, gantry speed was accelerated to 18°/s, limiting acquisition time to 10–20 s. Image quality, dosimetry and registration accuracy were compared with standard-CBCT (3°/s).

Methods and materials: For proof-of-concept, image quality was analyzed following customer acceptance tests, CT-dose index measured, and registration accuracy determined with an off-centered ball-bearing-phantom. A lung-tumor patient was simulated with differently shaped tumor-mimicking inlays in a thorax-phantom. Signal-to-noise-ratio, contrast-to-noise-ratio and geometry of the inlays quantified image quality. Dose was measured in representative positions. Registration accuracy was determined with inlays scanned in pre-defined positions. Manual, automatic (clinical software) and objective-automatic (in-house-developed) registration was performed on planning-CT, offsets between results and applied shifts were compared.

Results: Image quality of ultrafast-CBCT was adequate for high-contrast areas, despite contrast-reduction of ~80% due to undersampling. Dose-output was considerably reduced by 60–83% in presented setup; variations are due to gantry-braking characteristics. Registration accuracy was maintained better than 1 mm, mean displacement errors were 0.0 ± 0.2 mm with objective-automatic registration. Ultrafast-CBCT showed no significant registration differences to standard-CBCT.

Conclusions: This study of first tests with faster gantry rotation of 18°/s showed promising results for ultrafast high-contrast lung tumor CBCT imaging within single breath-hold of 10–20 s. Such fast imaging times, in combination with fast treatment delivery, could pave the way for intra-fractional combined imaging and treatment within one breath-hold phase, and thus mitigate residual motion and increase treatment accuracy and patient comfort. Even generally speaking, faster gantry rotation could set a benchmark with immense clinical impact where time matters most: palliative patient care, general reduction in uncertainty, and increase in patient throughput especially important for emerging markets with high patient numbers.

Respiratory motion management remains a major challenge in stereotactic body radiotherapy (SBRT) of inoperable lung tumors or lung metastases. Despite various clinically established approaches [1–4], optimization of motion management is still a demanding topic of research. While 4D-based strategies require least patient compliance, either the margin of the planning target volume (PTV) is enlarged due to internal motion inclusion (internal target volume, ITV), or treatment times rise due to gating strategies [5]. Deep-inspiration breath-hold (DIBH)-based treatment [6] minimizes the PTV margins and thus spares healthy tissue, while with flattening-filter-free delivery, treatment times can be further reduced to a few breath-holds (typically 10–20 s each) [7,8]. One remaining issue during the treatment of hypofractionated lung DIBH-SBRT is the long cone-beam CT (CBCT) imaging time for patient positioning of 1–4 min with repeated breath-hold, including 1–8 interruptions for breathing [9]. Furthermore, several studies determined repositioning errors of up to 1–2 mm between two breath-hold phases [10] and within one breath-hold [11,12].

* Corresponding author at: Department of Medical Physics and Bioengineering, Christchurch Hospital, Private Bag 4710, Christchurch 8140, New Zealand.
E-mail address: anna.arns@cdhb.health.nz (A. Arns).

https://doi.org/10.1016/j.radonc.2019.02.004
0167-8140/

A quasi-static situation with single breath-hold imaging and delivery would afford optimal imaging and delivery. To the best of our knowledge, our in-house developed ultrafast combined kilovoltage-Megavoltage (kV-MV) CBCT is the worldwide first technique which allows clinically applicable imaging within single breath-hold of 15 s [13–15].

With the release of IEC norm 60601-2-1 edition 3.0 in 2014 [16], linear accelerator (linac) rotations are allowed to be larger than 7°/s under specific conditions such as previous manufacturer risk analysis, pre-programmed rotation handling and the guarantee for the gantry to stop within 3°. Therefore, a clinical linac was modified to allow for a maximum rotation speed of 18°/s. With this maximum rotation speed of 3 rpm, 360° kV-only imaging could be performed within 20 s and thus single breath-hold kV-only CBCT could be possible for all available volume diameters.

This study provides the first pre-clinical evaluation regarding (I) image quality, (II) dosimetry and (III) registration accuracy with ultrafast gantry rotation speed of an otherwise clinical linear accelerator with (A) proof-of-concept commissioning and (B) phantom simulation of a lung tumor patient, and establishes the basis for clinical implementation.

Material and methods

A VersaHD linac equipped with a kV CBCT imaging XVI unit (Elekta AB, Stockholm, Sweden) was modified in the framework of a research agreement with an additional power supply for gantry rotation, modified control boards and research versions for the software of both linac and CBCT imaging system. CBCT detector and generator remained clinical with a pulse rate of 180 ms, resulting in 5.5 projections per second.

Initial safety checks

As part of the specific conditions required by IEC norm 60601-2-1 edition 3.0 [16], first tests on the gantry rotation to stop within 3° were performed. Results from signal to stop position were determined for gantry speed 6°/s, 12°/s and 18°/s. The gantry rotation was stopped externally via the interrupt button, the terminate button and a touchguard contact.

Setup imaging techniques

Two clinical imaging presets were analyzed and evaluated for conventional slow (3°/s) and ultrafast gantry speed (18°/s). For the Chest preset, image acquisition speed (without consideration of breathing interruptions for lung SBRT cases) was accelerated from 120 s (slow Chest-CBCT) to 20 s (fast Chest-CBCT). To further reduce imaging times, the asymmetric Head + Neck preset with centric detector position and 200° gantry rotation was also considered. Imaging speed was accelerated from 68 s (slow HN-CBCT) to 11 s (fast HN-CBCT). Thus, both ultrafast CBCT presets enable single-breath-hold imaging within 10–20 s. Details of the technical preset setups are shown in Table 1.

Image quality

Following customer acceptance tests [17], (I.A) image quality was analyzed regarding spatial resolution, uniformity, low contrast visibility and geometry with the CatPhan phantom (CTP503, The Phantom Laboratory, Salem, NY, USA) and a dedicated quality assurance preset (120 kV, 0.4mAs/frame, full rotation, high resolution) in slow (3°/s) and ultrafast (18°/s) gantry speed. Furthermore, (I.B) a lung tumor patient was simulated in the thorax phantom with four differently shaped tumor-mimicking inlays (transverse diameters between 6 and 15 mm) and signal-to-noise (SNR) as well as contrast-to-noise ratio (CNR) was evaluated for lung and tumor tissue. Additionally, the diameters of the tumor shapes were determined and differences to the sizes provided by the manufacturer were calculated. These measurements were performed for different clinical CBCT presets at different gantry speeds.

Dosimetry

Dose exposure was determined for all slow and ultrafast presets for (II.A) proof-of-concept in means of CT dose index (CTDI) [1,15,18] and (II.B) simulation of a lung tumor patient with a thorax phantom (model 002LFC, CIRS, Norfolk, VA, USA) [15]. The weighted CTDI was measured in an appropriate 40 cm long QA phantom and a 10 cm long ionization chamber (Type 30009, PTW Freiburg GmbH, Freiburg, Germany). The simulated lung tumor in the thorax phantom was defined in the lower left lung of the phantom, which was also the position of the isocenter. Dose measurements were performed in six representative tissues: tumor in left lung, center of left and right lung, upper periphery, spinal cord and body center. A flexible cylindrical ionization chamber (Type 31013, 0.3 cm^3 sensitive volume, PTW Freiburg GmbH, Freiburg, Germany), calibrated in air kerma for kV-range (50-150kVp) was used. The dose measurements were calibrated and corrected according to the AAPM TG61 protocol [19].

Registration accuracy

An off-center positioned ball-bearing-phantom (Elekta AB) was used to evaluate the (III.A) automatic registration accuracy in means of proof-of-concept. For evaluation of (III.B) registration accuracy for a simulated lung tumor patient, four different tumor-mimicking inlays in a thorax phantom were scanned sequentially at 10 different pre-defined positions. High-precision phantom positioning in right–left (RL), anterior–posterior (AP) and cranio-caudal (CC) directions was assured by optical tracking with a step-width of 0.01 mm (Clarity, Elekta AB). Registration to planning-CT was applied offline with three different methods: (1) manual by two experienced clinicians, (2) clinical automatic XVI software [20], and (3) in-house developed fully-automated and independent registration framework programmed with MATLAB [14]. The offsets between the registration results and the known isocenter shifts were determined and compared. To evaluate

Table 1
Technical specifications for different CBCT imaging presets and gantry rotation speeds.

CBCT preset	Head + Neck preset		Chest preset	
	slow HN-CBCT	fast HN-CBCT	slow Chest-CBCT	fast Chest-CBCT
Output characteristics	100 kV, 0.1mAs/frame		120 kV, 0.4 mAs/frame	
Panel position	Centered (S)		Off-centered (M)	
Acquisition interval	−135° to 70°		−180° to 180°	
Filter, collimator	F0 (empty), S20 (27.6 cm × 27.6 cm)		F1 (bow-tie), M20 (27.6 cm × 42.6 cm)	
Imaging speed	3°/s	18°/s	3°/s	18°/s
Acquisition time	68 s	11 s	120 s	20 s
Nominal dose	1 mGy	~0.17 mGy	5 mGy	~0.83 mGy

statistical significance between imaging speeds, paired difference Wilcoxon's Signed Rank Tests were performed with MATLAB [14,21]. Null hypothesis indicated a zero mean of the difference between the paired samples, with significance level 5%.

Results

Prior to the comparison study between ultrafast (18°/s) and conventional, clinical (3°/s) CBCT presets, rotational detector center fluctuations in terms of so-called flexmaps were acquired and analyzed for different gantry speeds. Offsets to the clinical flexmap (6°/s gantry speed) were in average below 0.05 mm, thus the clinical flexmap was chosen as default for all gantry speeds.

Initial safety checks on the gantry rotation to stop showed that the requirements by IEC norm 60601-2-1 edition 3.0 [16] are met. From signal to stop position, the gantry stops within in average 0.3° for gantry rotation speed 6°/s, and in average 1.0° for gantry rotation speed 18°/s. Signals tested were the interrupt button, the terminate button and a touchguard contact. More detailed evaluation of movement stop still has to be performed by the vendor as part of their risk analysis.

Proof-of-principle (I.A) image quality commissioning tests [17] with a dedicated QA imaging preset result in a spatial resolution of 12 line pairs per centimeter for both gantry speeds, corresponding to a visible rod gap of 0.42 mm [22] and well within specification. Low contrast visibility between water and fat material was 2.7% for slow and 8% for ultrafast gantry speed, and thus failed the specification due to undersampling, i.e. one projection every ~3° only. Uniformity and geometry tests passed the customer acceptance criteria for both speeds (Table 2(a) and Fig. 1(a)).

The results for (I.B) SNR and CNR of the high-density tumor-mimicking inlays (averaged) and lung tissue in a thorax phantom are presented in Table 2(b). The SNR was reduced by 7–11% respective 34–45% with ultrafast gantry rotation. The CNR between tumor and lung material was reduced up to 78% due to undersampling, however, image quality for tumor localization in this high contrast area was still sufficient. Table 2(c) shows the comparison of the measured geometric body shapes of the tumor-mimicking inlays in transverse direction and the respective diameters provided by the manufacturer. The mean difference was better than 1 mm for all presets and speeds, with a maximum difference of 2 mm. An example of transverse profiles through the body of a tumor-mimicking ball-shaped inlay for all CBCT presets is shown in Fig. 1(b).

Since both CBCT detector and generator were not adapted, dose is expected to be reduced by a factor of 6 for faster gantry rotation. Table 3(a) shows the (II.A) separate measurements for the CTDI, the resulting weighted $CTDI_w$ and the ratio between ultrafast and slow CBCT presets. With ultrafast gantry rotation, the measured CTDI-values were reduced by factors of 2.5–5.8 (60.2–83.7%). (II.B) Measurement results and ratios between ultrafast and slow CBCTs in different positions of the thorax phantom are shown in Table 3(b). Gantry acceleration led to a measured dose reduction of 3.4–5.7 (70.9–82.3%). Lowest dose-reductions occurred at the start and stop position of the gantry rotation (i.e. 160° for HN-CBCT and 270° for Chest-CBCT) due to gantry braking characteristics.

The (III.A) proof-of-concept registration accuracy test performed with a translationally off-center positioned ball-bearing-phantom showed a mean displacement error of (-0.4 ± 0.1)mm, with maximum/minimum offsets of −0.3/−0.5 mm for all CBCT presets and different gantry speeds.

For the (III.B) registration accuracy study of a simulated lung tumor case, the systematic error of the 10 random pre-selected translational isocenter shifts up to 19 mm was reduced to 0.05 mm with optical tracking [14,23]. The stochastic mean displacement error for all tumor-mimicking inlays, HN- and Chest-CBCT presets, isocenter shifts and translational directions (RL, AP, CC) was with (1) manual registration (0.0 ± 0.2)mm for both gantry speeds. The maximum offsets were −0.8/0.7 mm for slow, and −0.7/0.9 mm for ultrafast imaging speed. With the (2) clinical software, the mean registration accuracy was (0.0 ± 0.4)mm for both gantry speeds, with maximum detection errors of −0.9/1.0 mm for slow, and −1.0/1.2 mm for ultrafast imaging speed. Objective evaluation was achieved with the (3) self-developed fully-automatic registration method by applying an identical region of interest around the tumor-shapes for all scanned volumes [14].

Table 2
Image quality comparison between slow and ultrafast CBCT presets: (a) customer acceptance results with CatPhan phantom, (b) lung-tumor simulation in thorax phantom: SNR and CNR for lung and tumor-mimicking tissue, (c) thorax phantom: differences between measured transverse diameters of tumor-mimicking inlay bodies and corresponding dimensions provided by manufacturer.

(a): Image quality – CatPhan QA

		Specification	QA preset (120 kV, S20 collimator (centric), 0.1mAs/frame, 360° rotation)	
Gantry speed [°/s]		3	3	18
Uniformity [%]		<1.5	0.4	1.1
Low Contrast Visibility [%]		<3.0	2.7	8.0
Spatial resolution [lp/cm]		>10	12	12
Geometry [mm]	Transverse	117.0 ± 1.0	116.5	116.5
	Sagittal	110.0 ± 1.0	110.0	110.0

(b): Image quality – thorax phantom – simulation lung cancer patient: SNR and CNR for lung and tumor-mimicking tissue

Differences between slow and fast CBCT presets	slow vs. fast HN-CBCT	slow vs. fast Chest-CBCT
Signal-to-noise ratio in tumor inlay [%]	7.4	10.5
Signal-to-noise ratio in lung [%]	33.7	44.5
Contrast-to-noise ratio between tumor inlay and lung [%]	77.8	74.3

(c): Image quality – thorax phantom – simulation lung cancer patient: measured diameters of different tumor-mimicking inlays compared to sizes provided by manufacturer

	Head + Neck preset		Chest preset	
Difference measurement vs. manufacturer size	slow HN-CBCT	fast HN-CBCT	slow Chest-CBCT	fast Chest-CBCT
Mean ± std dev [mm]	−0.5 ± 0.7	−0.8 ± 0.8	−0.4 ± 0.5	−0.4 ± 0.5
Min/max [mm]	−2.0/0.0	−2.0/0.0	−1.0/0.0	−1.0/0.0

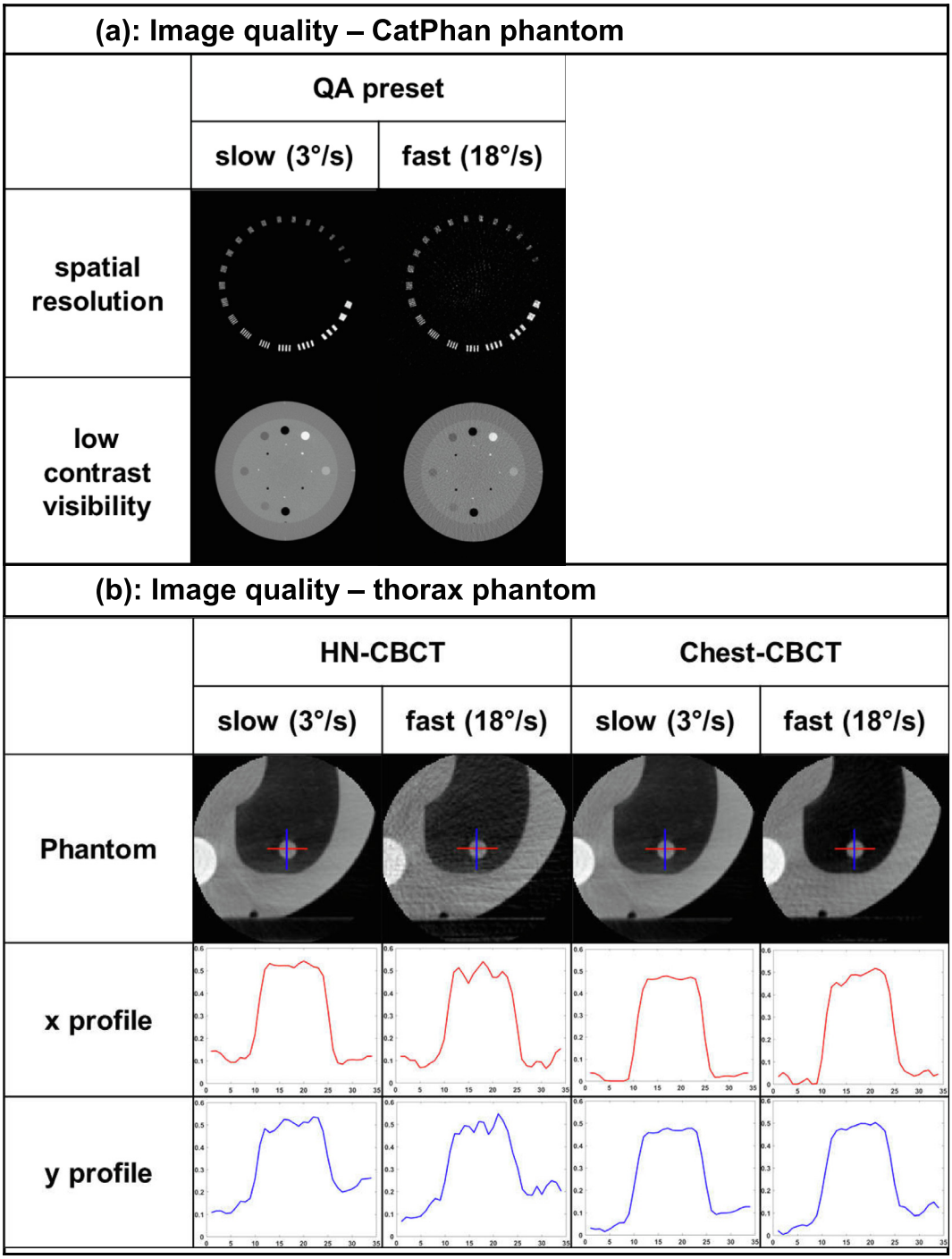

Fig. 1. Image quality comparison between slow and ultrafast CBCT presets: (a) customer acceptance tests with CatPhan phantom (spatial resolution and low contrast visibility) with a dedicated QA preset, and (b) representative profiles through ball-shaped tumor-mimicking inlay body in a thorax phantom.

Here, the mean displacement error was (0.0 ± 0.2)mm for both imaging speeds, with maximum offsets of −0.5/0.7 mm for slow and −0.6/0.7 mm for ultrafast imaging speed.

For qualitative visual evaluation, Fig. 2(a) shows an exemplary registration result of CBCT scans in slow and ultrafast imaging speed onto the planning-CT of a star-shaped tumor-mimicking inlay, performed with the (3) objective, in-house developed automatic registration method. Fig. 2(b) demonstrates the quantitative evaluation by means of box-and-whisker-diagrams, which give an overview of detection error distributions, separated for different CBCT presets and imaging speeds, different registration methods and translational directions (RL, AP, CC). All three registration methods followed the same trend, i.e. both automatic registration results validated the objective performance of manual registration by the experienced clinicians. Table 4 shows the corresponding mean detection errors (±standard deviation) as well as minimum and maximum values. Technically it is expected that registrations with different imaging speeds show significant registration differences. Paired difference test between slow and ultrafast imaging speed of each CBCT preset however showed mostly no significant statistical differences (p = 0.001–0.926). For the few significant differences there is no clear trend explainable. Absolute differences

Table 3
Calibrated dose measurement values for (a) weighted CTDI and (b) lung tumor patient simulation with the thorax phantom, for two different CBCT presets with slow and ultrafast gantry speed, as well as the ratio between slow and ultrafast imaging speed.

(a): CT dose index determination for different CBCT presets and corresponding gantry speeds

Preset		$CTDI_c$ [mGy]	$CTDI_{p,0°}$ [mGy]	$CTDI_{p,90°}$ [mGy]	$CTDI_{p,180°}$ [mGy]	$CTDI_{p,270°}$ [mGy]	$CTDI_w$ [mGy]
Head + Neck CBCT	Slow HN-CBCT	1.06	1.54	1.80	0.95	0.64	1.23
	Fast HN-CBCT	0.23	0.27	0.39	0.28	0.14	0.27
	Ratio	*4.6*	*5.7*	*4.6*	*3.4*	*4.7*	*4.6*
Chest CBCT	Slow Chest-CBCT	4.40	6.61	6.11	5.96	6.55	6.31
	Fast Chest-CBCT	0.98	1.08	1.05	1.16	2.61	1.47
	Ratio	*4.5*	*6.1*	*5.8*	*5.2*	*2.5*	*4.3*

(b): Thorax phantom: dose measurements for different CBCT presets and corresponding gantry speeds in different body positions

	Head + Neck preset			Chest preset		
	slow HN-CBCT [mGy]	fast HN-CBCT [mGy]	Ratio	slow Chest-CBCT [mGy]	fast Chest-CBCT [mGy]	Ratio
1 – Tumor – lower left lung	1.2	0.3	*4.5*	10.2	1.8	*5.7*
2 – Upper left lung	1.4	0.3	*4.8*	10.0	1.8	*5.7*
3 – Right lung	0.3	0.1	*3.7*	5.1	1.5	*3.4*
4 – Upper center	0.8	0.2	*4.9*	6.4	1.2	*5.4*
5 – Spinal cord	0.4	0.1	*3.9*	6.2	1.4	*4.4*
6 – Body center	0.7	0.1	*4.9*	6.1	1.4	*4.4*

between registration results of different imaging speeds for all presets and directions are in average (-0.01 ± 0.12)mm, with maximum differences of 0.6 mm. In overall conclusion, registration detection errors were well below tolerance level of 1 mm.

Discussion

Ultrafast (single breath-hold) CBCT imaging for patient positioning is not only desirable in case of DIBH-SBRT treatment of e.g. lung, liver or breast tumors, but also for other tumor sites where a reduction in patient-on-couch-time is crucial, i.e. for palliative cases such as high-contrast areas in the pelvic area (bones) or intracranial lesions. With the legal allowance to rotate the gantry faster than 7°/s under specific conditions [16], ultrafast gantry rotation is realizable on a commercial C-arm linear accelerator with some hardware modifications such as faster detector readout and a more powerful X-ray generator. For high-contrast areas, it could already be applied in the current setup.

This study analyzed the clinical feasibility of 18°/s CBCT imaging speed (3 rpm) in comparison to clinically established CBCT presets with gantry speed 3°/s (0.5 rpm) by means of (A) proof-of-concept commissioning tests regarding (I) image quality, (II) dosimetry and (III) registration accuracy. Furthermore, the treatment site profiting most from high-speed imaging within single breath-hold range, i.e. hypofractionated DIBH-SBRT of lung tumors, was evaluated more detailed by (B) simulating a lung cancer patient with a thorax phantom and 4 tumor-mimicking inlays regarding (I)–(III), respectively.

In summary, both (A) proof-of-principle commissioning tests and (B) phantom simulation of a lung tumor patient, (I) image quality was maintained, only contrast was out of tolerance. This is due to undersampling in the presented setup with the clinical X-ray pulse rate of 180 ms and thus acquisition of 5.5 projections per second, i.e. one projection every ∼3°. However, image quality was still sufficient for high-contrast areas such as lung tumors, or palliative cases where a bony matching is precise enough and where reduction in patient-on-couch-time is of utmost importance. (II) Dose output was considerably reduced with ultrafast gantry rotation in the presented setup. Essential however is that the (III) registration accuracy was maintained below 1 mm and detection errors of ultrafast and slow CBCT showed no statistically significant differences between registration results with different imaging speeds, whereas imaging time was dramatically reduced.

Limitations detected in this survey could be attributed to the fact, that in these first tests, the only modification to the clinical linac was hardware-based by attaching an additional power supply for the gantry engine. For high-contrast areas such as lung tumors, image quality would be sufficient with the setup presented in this study. For broader applications on other tumor entities, further hardware improvements on projection acquisition and thus image quality would be necessary before clinical implementation. Namely, the CBCT detector readout and pulses per second given by the generator would have to be increased, resulting in more projections per second and degree, coinciding with higher imaging dose, which would then be comparable to current clinical imaging dose with slower gantry speed. Furthermore, software-related issues would have to be solved, such as synchronizing frame grabbing with gantry braking characteristics, which lead to lower dose reduction and stripe artifacts at start- and end-angle of the image acquisition. Eventually, robustness tests such as gantry collision stop, detector tilt and flexmap response would have to be further investigated.

Regardless of these minor issues, ultrafast single breath-hold kV-CBCT for lung cancer was proven to be clinically applicable and a promising alternative to our in-house developed combined kV-MV single breath-hold CBCT imaging technique [13–15] or other clinically established slower kV-CBCT imaging techniques, which require 1–8 repeated breath-holds in order to acquire the necessary number of projections. Koshani et al. [10] already proposed the weak point of residual repositioning errors of 1–2 mm between two breath-hold phases and there are recent data on intra-breath-hold residual motion [12]. Also in regard to faster treatment delivery, multiple studies were performed in recent years evaluating the dosimetric impact of higher dose rates and flattening-filter-free beams on interplay effects in intra-fractional motion. Bortfeld et al. [24] and Ong et al. [25] conclude that in case of organ motion, more treatment fractions/more breath-holds would lead to a more solid target dose coverage. The probability distribution to hit the target is closest to a Gaussian distribution the more fractions are applied.

Therefore, with constant novel developments, the ultimate goal of lung cancer radiation therapy would be to not have to deal with (intrafractional) motion management at all by simply treating the patient within such a short time, that both imaging and treatment could be accomplished in one breath-hold phase of 20–30 s. Kemmerling et al. [26] stated, the simplest solution for motion management would be, to "deliver the treatment so rapidly that the

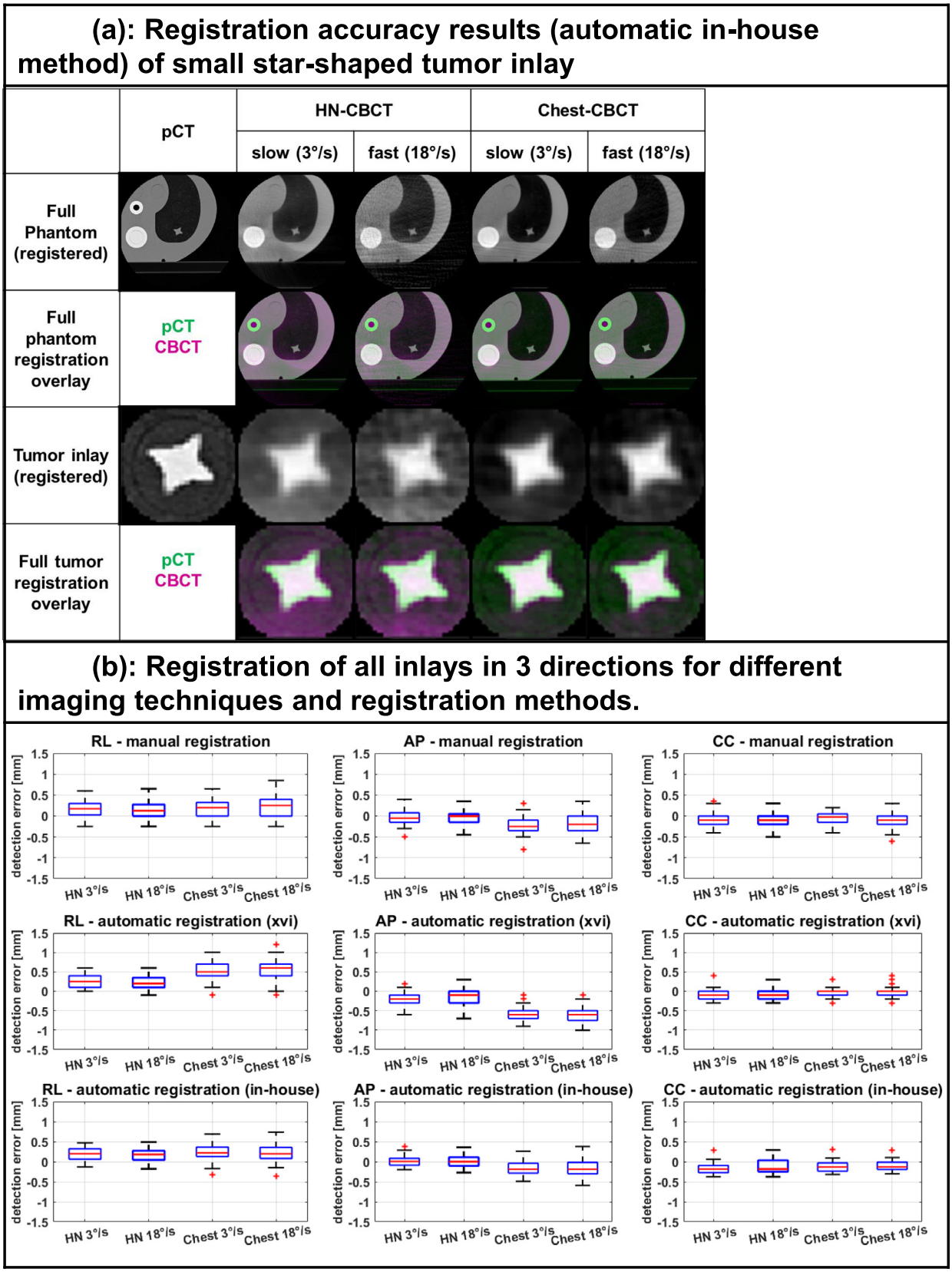

Fig. 2. Registration accuracy: (a) quantitative evaluation with representative slices of the star-shaped tumor-mimicking inlay with the automatic in-house developed registration method, and (b) qualitative evaluation with box-whisker-diagrams, showing the detection errors for all presets with different gantry speeds in all translational directions (RL, AP, CC) and all registration methods (manual, automatic clinical and objective, automatic in-house developed method).

Table 4
Registration accuracy: detection errors for different imaging presets and gantry speeds as well as registration methods, representing the average over 4 tumor-mimicking inlays and 10 pseudo-random isocenter shifts in translational directions (RL, AP, CC) and corresponding maximum/minimum detection errors.

Detection error: mean ± std (min/max)		Head + Neck preset		Chest preset	
		Slow HN-CBCT	Fast HN-CBCT	Slow Chest-CBCT	Fast Chest-CBCT
Manual registration	RL [mm]	0.2 ± 0.2 (0.6/-0.3)	0.1 ± 0.2 (0.7/−0.3)	0.2 ± 0.2 (0.7/−0.3)	0.2 ± 0.2 (0.9/−0.3)
	AP [mm]	0.0 ± 0.2 (0.4/−0.5)	0.0 ± 0.2 (0.4/−0.5)	−0.2 ± 0.2 (0.3/−0.8)	−0.2 ± 0.2 (0.4/−0.7)
	CC [mm]	−0.1 ± 0.2 (0.4/−0.4)	−0.1 ± 0.2 (0.3/−0.5)	0.0 ± 0.1 (0.2/−0.4)	−0.1 ± 0.2 (0.3/−0.6)
Automatic registration (XVI)	RL [mm]	0.3 ± 0.2 (0.6/0.0)	0.2 ± 0.2 (0.6/−0.1)	0.5 ± 0.2 (1.0/−0.1)	0.6 ± 0.3 (1.2/−0.1)
	AP [mm]	−0.2 ± 0.2 (0.2/−0.6)	−0.1 ± 0.2 (0.3/−0.7)	−0.6 ± 0.2 (-0.1/−0.9)	−0.6 ± 0.2 (-0.1/−1.0)
	CC [mm]	−0.1 ± 0.1 (0.4/−0.3)	−0.1 ± 0.2 (0.3/−0.3)	0.0 ± 0.1 (0.3/−0.3)	0.0 ± 0.1 (0.4/−0.3)
Automatic registration (in-house)	RL [mm]	0.2 ± 0.2 (0.5/−0.1)	0.2 ± 0.2 (0.5/−0.2)	0.2 ± 0.2 (0.7/−0.3)	0.2 ± 0.2 (0.7/−0.4)
	AP [mm]	0.0 ± 0.1 (0.4/−0.2)	0.0 ± 0.2 (0.4/−0.3)	−0.2 ± 0.2 (0.3/−0.5)	−0.2 ± 0.2 (0.4/−0.6)
	CC [mm]	−0.2 ± 0.1 (0.3/−0.4)	−0.1 ± 0.2 (0.3/−0.4)	−0.1 ± 0.1 (0.3/−0.3)	−0.1 ± 0.1 (0.3/−0.3)

patient has no time to move". They proposed the idea of extremely rapid radiotherapy, however with very high-energy electron (VHEE) beams: first, a helical CT for gross registration of the tumor position of the day is performed in deep inspiration breath-hold. Thereafter, within a single breath-hold phase, single projection acquisition and treatment with VHEE can be completed within one breath-hold. However, proper matching of projection and daily helical CT, as well as plan adaptation of the dose distribution of the initial planning-CT are crucial prerequisites for successful accomplishment and still work in progress.

Ultrafast gantry rotation speed of a clinical linac paves the way to adapt their approach of combining imaging and treatment (sequence) within one breath-hold to a clinical C-arm linac, and thus mitigating the effect of breathing motion between separate imaging and treatment breath-hold phases [10,11,27]. Besides those visions of future combined imaging and treatment techniques to mitigate breathing motion, ultrafast CBCT imaging could already today set a benchmark with immense clinical impact. Furthermore, for palliative cases, reducing on-couch time is of great importance.

Conclusion

With recent legal allowance to accelerate the linac gantry rotation speed up to 18°/s (3 rpm), ultrafast single breath-hold CBCT for lung-SBRT is achievable within 10–20 s (respective 180°–360° imaging arc). This comparison study between ultrafast kV-CBCT (18°/s) and conventional, clinical kV-CBCT (3°/s) provides a good overview of proof-of-principle commissioning evaluation and lung-cancer specific patient simulation regarding image quality, dosimetry and registration accuracy. Overall, this first setup of just accelerated gantry speed shows promising results for high-contrast areas: dramatically reduced imaging time for considerably less dose, sufficient image quality and maintained registration accuracy compared to conventional CBCT imaging. Therefore, ultrafast kV-CBCT lung tumor imaging within single breath-hold of 10–20 s would be clinically applicable, and paves the way for future intra-fractional combined imaging and treatment within one breath-hold phase. Generally speaking, this approach of faster gantry rotation could benchmark not only ultrafast imaging for all anatomical regions, but also accelerate the treatment delivery.

Acknowledgements

The authors would like to thank Colin Winfield, John Allen, Gustav Meedt, Antonio Cossu and Uwe Gros from Elekta for their continuous support of this project. The project received funding by an Elekta AB, Sweden research grant.

Conflicts of interest/disclosures

Dr. Arns reports grants and personal fees from Elekta during the conduct of the study.

Dr. Wertz reports grants from Elekta during the conduct of the study; and grants and personal fees from Elekta, as well as grants and personal fees from IBA outside the submitted work.

Dr. Boda-Heggemann has nothing to disclose.

Dr. Schneider reports grants from Elekta during the conduct of the study; personal fees from Carl-Zeiss Meditech as well as personal fees from Elekta outside the submitted work.

Dr. Blessing has nothing to disclose.

Dr. Abo-Madyan reports other from Elekta, other from Carl-Zeiss Meditech, and other from Merck-Serono outside the submitted work.

Mr. Steil reports grants from Elekta during the conduct of the study.

Dr. Wenz reports grants and non-financial support from Elekta during the conduct of the study; grants, personal fees and non-financial support from Carl Zeiss Meditech, grants and non-financial support from Nucletron, personal fees from Celgene, personal fees from Ipsen outside the submitted work.

Dr. Fleckenstein reports grants and personal fees from Elekta during the conduct of the study; personal fees from Siemens outside the submitted work.

References

[1] Ding GX, Alaei P, Curran B, et al. Image guidance doses delivered during radiotherapy: quantification, management, and reduction: Report of the AAPM Therapy Physics Committee Task Group 180. Med Phys 2018;45(5):e84–99.
[2] Keall PJ, Mageras GS, Balter JM, et al. The management of respiratory motion in radiation oncology report of AAPM Task Group 76. Med Phys 2006;33(10):3874–900.
[3] Chi A, Nguyen NP, Komaki R. The potential role of respiratory motion management and image guidance in the reduction of severe toxicities following stereotactic ablative radiation therapy for patients with centrally located early stage non-small cell lung cancer or lung metastases. Front Oncol 2014;4:1–12.
[4] Alaei P, Spezi E. Imaging dose from cone beam computed tomography in radiation therapy. Phys Medica 2015;31(7):647–58.
[5] Wolthaus JWH, Sonke J-J, van Herk M, et al. Comparison of different strategies to use four-dimensional computed tomography in treatment planning for lung cancer patients. Int J Radiat Oncol Biol Phys 2008;70(4):1229–38.
[6] Boda-Heggemann J, Knopf A-C, Simeonova-Chergou A, et al. Deep inspiration breath hold – based radiation therapy: a clinical review. Int J Radiat Oncol Biol Phys 2016;94(3):478–92.
[7] Boda-Heggemann J, Mai S, Fleckenstein J, et al. Flattening-filter-free intensity modulated breath-hold image-guided SABR (Stereotactic ABlative Radiotherapy) can be applied in a 15-min treatment slot. Radiother Oncol 2013;109:505–9.
[8] Navarria P, Ascolese AM, Mancosu P, et al. Volumetric modulated arc therapy with flattening filter free (FFF) beams for stereotactic body radiation therapy (SBRT) in patients with medically inoperable early stage non small cell lung cancer (NSCLC). Radiother Oncol 2013;107(3):414–8.

[9] Boda-Heggemann J, Fleckenstein J, Lohr F, et al. Multiple breath-hold CBCT for online image guided radiotherapy of lung tumors: simulation with a dynamic phantom and first patient data. Radiother Oncol 2011;98(3):309–16.
[10] Koshani R, Balter JM, Hayman JA, et al. Short-term and long-term reproducibility of lung tumor position using active breathing control (ABC). Int J Radiat Oncol Biol Phys 2006;65(5):1553–9.
[11] Blessing M, Hofmann J, Vogel L, et al. An offline technique to evaluate residual motion of the diaphragm during deep inspiratory breath-hold from cone-beam CT datasets. Strahlenther Onkol 2018;194(9):855–60.
[12] Vogel L, Sihono DSK, Weiss C, et al. Intra-breath-hold residual motion of image-guided DIBH liver-SBRT: an estimation by ultrasound-based tracking correlated with diaphragm position in CBCT. Radiother Oncol 2018;129(3):441–8.
[13] Blessing M, Arns A, Wertz H, et al. Automated ultrafast kilovoltage-megavoltage cone-beam CT for image guided radiotherapy of lung cancer: system description and real-time results. Z Med Phys 2018;28:110–20.
[14] Arns A, Blessing M, Fleckenstein J, et al. Towards clinical implementation of ultrafast combined kV-MV CBCT for IGRT of lung cancer. Strahlenther Onkol 2016;192(5):312–21.
[15] Arns A, Blessing M, Fleckenstein J, et al. Phantom-based evaluation of dose exposure of ultrafast combined kV-MV-CBCT towards clinical implementation for IGRT of lung cancer. PLoS ONE 2017;12(11):e0187710.
[16] IEC60601-1-2-1:2009+AMD1:2014, Medical electrical equipment – Part 2-1: Particular requirements for the basic, safety and essential performance of electron accelerators in the range 1MeV to 50MeV. IEC, Geneva, Switzerland; 2014
[17] Elekta XVI. R5.0 Customer Acceptance Tests. Crawley, UK: Elekta; 2015.
[18] Murphy MJ, Balter J, Balter S, et al. The management of imaging dose during image-guided radiotherapy: Report of the AAPM Task Group 75. Med Phys 2007;34(10):4041–63.
[19] Ma C-M, Coffey CW, DeWerd LA, et al. AAPM protocol for 40–300 kV X-ray beam dosimetry in radiotherapy and radiobiology. Med Phys 2001;28(6):868–93.
[20] Hristov DH, Fallone BG. A grey-level image alignment algorithm for registration of portal images and digitally reconstructed radiographs. Med Phys 1996;23(1):75–84.
[21] Wilcoxon F. Individual comparisons of grouped data by ranking methods. Biometrics Bull 1945;1(6):80–3.
[22] CatPhan 500 and 600 Manual. Salem, NY, USA; 2009.
[23] Wiles AD, Thompson DG, Frantz DD. Accuracy assessment and interpretation for optical tracking systems. Med. Imaging 2004 Vis. Image-guided Preced. Display. Proc. SPIE. 2004;5367:421-32.
[24] Bortfeld T, Jokivarsi K, Goitein M, et al. Effects of intra-fraction motion on IMRT dose delivery: statistical analysis and simulation. Phys Med Biol 2002;47:2203–20.
[25] Ong CL, Dahele M, Slotman BJ, et al. Dosimetric impact of the interplay effect during stereotactic lung radiation therapy delivery using flattening filter-free beams and volumetric modulated arc therapy. Int J Radiat Oncol Biol Phys 2013;86:743–8.
[26] Cherry Kemmerling EM, Wu M, Yang H, et al. Optimization of an on-board imaging system for extremely rapid radiation therapy. Med Phys 2015;42(11):6757–67.
[27] Ohlmann C, Schneider F, Arns A, et al. PO-1001: Implementation and experimental verification of a faster gantry rotation in lung SBRT. Radiother Oncol 2018;127:S558.